Biomol NMR Assign (2014) 8:349–356
DOI 10.1007/s12104-013-9515-1

ARTICLE

Solid-state NMR sequential assignments of the amyloid core of full-length Sup35p

Anne K. Schütz · Birgit Habenstein · Nina Luckgei · Luc Bousset · Yannick Sourigues · Anders B. Nielsen · Ronald Melki · Anja Böckmann · Beat H. Meier

Received: 12 April 2013 / Accepted: 1 August 2013 / Published online: 14 August 2013

Abstract Sup35p is a yeast prion and is responsible for the [*PSI*$^+$] trait in *Saccharomyces cerevisiae*. With 685 amino acids, full-length soluble and fibrillar Sup35p are challenging targets for structural biology as they cannot be investigated by X-ray crystallography or NMR in solution. We present solid-state NMR studies of fibrils formed by the full-length Sup35 protein. We detect an ordered and rigid core of the protein that gives rise to narrow and strong peaks, while large parts of the protein show either static disorder or dynamics on time scales which interfere with dipolar polarization transfer or shorten the coherence lifetime. Thus, only a small subset of resonances is observed in 3D spectra. Here we describe in detail the sequential assignments of the 22 residues for which resonances are observed in 3D spectra: their chemical shifts mostly corresponding to β-sheet secondary structure. We suspect that these residues form the amyloid core of the fibril.

Keywords Sup35p · Fibrils · Solid-state NMR · Assignments · Secondary structure

Anne K. Schütz, Nina Luckgei, Birgit Habenstein, and Luc Bousset have contributed equally to this work.

A. K. Schütz · A. B. Nielsen · B. H. Meier (✉)
Physical Chemistry, ETH Zürich, Wolfgang-Pauli-Strasse 10, 8093 Zurich, Switzerland
e-mail: beme@ethz.ch

B. Habenstein · N. Luckgei · A. Böckmann (✉)
Institut de Biologie et Chimie des Protéines, UMR 5086 CNRS/Université de Lyon 1, 7 passage du Vercors, 69367 Lyon, France
e-mail: a.bockmann@ibcp.fr

L. Bousset · Y. Sourigues · R. Melki (✉)
Laboratoire d'Enzymologie et Biochimie Structurales, UPR 3082 CNRS, Avenue de la Terrasse, 91198 Gif-sur-Yvette, France
e-mail: melki@lebs.cnrs-gif.fr

Biological context

Sup35p is a yeast prion from *Saccharomyces cerevisiae* and is at the origin of the [*PSI*$^+$] phenotype (Cox 1965; Wickner et al. 1995). It contains 685 amino acids and consists of three domains. The N-terminal domain (N-domain), comprising residues 1–123, is rich in glutamine and asparagine residues. It has been proposed that the N-domain plays a critical role in prion propagation (DePace et al. 1998). The middle domain (M-domain) with unknown function mainly consists of highly charged residues. The C-terminal domain, spanning residues 254–685, has GTPase activity and is involved in translation termination (Stansfield et al. 1995). Since Sup35p is not infectious for human beings, it is well suited as a model system to gain deeper insight into the structural features of prion proteins.

Until now most of the structural and functional studies concerning Sup35p have been performed on small fragments of the N-domain, as for example Sup35p 7–13, or on the N-domain by itself or together with the M-domain, Sup35pN and Sup35pNM, respectively (Nelson et al. 2005; Krishnan and Lindquist 2005; Shewmaker et al. 2006; van der Wel et al. 2006, 2007; Toyama et al. 2007; van der Wel et al. 2010; Vranken et al. 2005). Sup35p and Sup35pNM both form self-seeding amyloid fibrils in vivo and in vitro under physiological pH and salt concentrations. However, it has been suspected that the two proteins differ in their assembly and infection properties (Krzewska et al. 2007). The assignment of Sup35pNM is described in a companion paper (Luckgei et al. 2013b). A detailed comparison and a biophysical interpretation will be presented elsewhere (Luckgei et al. 2013a).

Solid-state NMR spectroscopy has evolved into a powerful tool to structurally investigate protein fibrils (Tycko 2006; Wasmer et al. 2008; Heise et al. 2008; Paravastu et al. 2008; Loquet et al. 2009; van Melckebeke et al. 2010; Böckmann and Meier 2010; Debelouchina et al. 2010; Loquet et al. 2010; van der Wel et al. 2010; Lewandowski et al. 2011; Comellas et al. 2011; Gath et al. 2012; Fitzpatrick et al. 2013). Here we show that even large proteins like Sup35p are amenable to solid-state NMR studies and present the sequential assignments of the resonances visible in 3D correlation spectra, which are all located within the first 30 residues of the protein.

Methods and experiments

Protein expression and purification; sample preparation

Sup35p expression and purification were done as described in Krzewska and Melki (2006), Krzewska et al. (2007). For convenience of the reader, we summarize it in the following. The proteins were expressed with an N-terminal His-tag (for the full amino acid sequence see Fig. 1) and purified as described, using M9 medium with ^{13}C and ^{15}N labeling. To form fibrillar aggregates, Sup35p (in 20 mM Tris HCl, pH 8.0, 200 mM NaCl, 5 % glycerol, 5 mM β-mercaptoethanol, 1 mM ATP, 1 mM GTP, 10 mM $MgCl_2$) was incubated at 10 °C under orbital shaking at 30 rpm, 0.5 cm amplitude, for 3 weeks. The fibrils were spun at 100,000*g* in a TL-100 tabletop centrifuge for 20 min at 4 °C. The pellets were resuspended in distilled water, washed twice, and filled into 3.2 mm rotors by ultracentrifugation as described (Böckmann et al. 2009).

NMR spectroscopy

2D and 3D experiments were used for assignments: 2D DARR and DREAM, 3D NCACB, NCACO, NCACX, NCOCA, NCOCX, CANCO and CCC. The procedure is described in detail in references Habenstein et al. (2011) and Schuetz et al. (2010). 3D spectra were recorded for 2–6 days each (details in Table 1). Resonances were

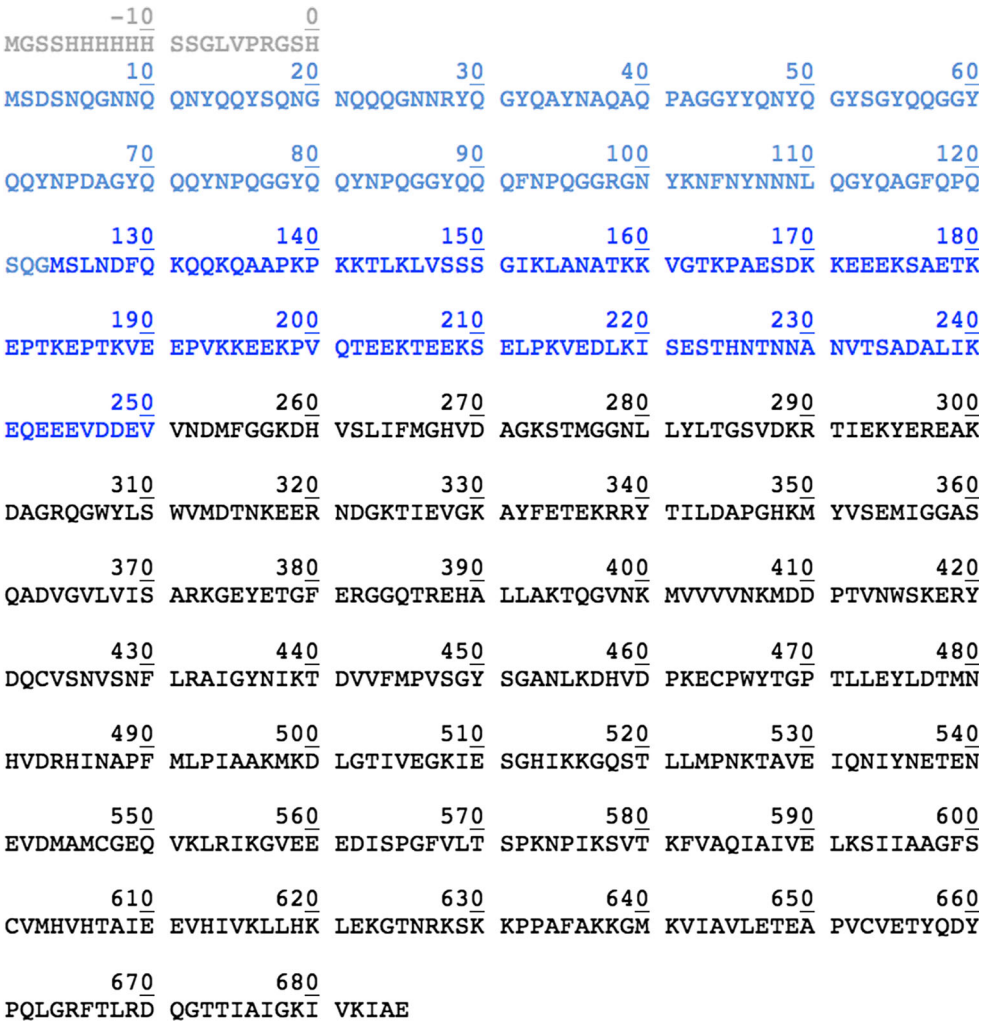

Fig. 1 Amino-acid sequence of Sup35p, including the purification tag added at the N-terminus (*in grey*). The N domain is shown in *light blue*, and the M domain in *deep blue*, and the C-terminal domain in *black*

Table 1 Experimental parameters

a

Experiment	DARR	DREAM	NCA	NCACB	NCACO	NCOCA
MAS frequency (kHz)	18.0	17.5	17.5	17.5	17.5	17.5
Transfer 1	HC-CP	HC-CP	HN-CP	HN-CP	HN-CP	HN-CP
Field (kHz)-^{1}H	65.5	72.6	54.4	54.4	58.3	59.0
Field (kHz)-X	55.5	62.3	40.6	41.6	45.6	45.6
Shape	Tangent ^{1}H	Tangent ^{1}H	Tangent ^{1}H	Tangent ^{1}H	Tangent ^{1}H	Tangent ^{1}H
^{13}C carrier (ppm)	55.6	55.6	–	–	–	–
Time (ms)	0.5	0.5	0.8	0.8	0.9	0.8
Transfer 2	DARR	DREAM	NC-CP	NC-CP	NC-CP	NC-CP
Field (kHz)-^{1}H	5.5	102	102	115	102	102
Field (kHz)-^{13}C	–	8.3	10.6	12.5	10.6	10.8
Field (kHz)-^{15}N	–	–	7.5	6.5	7.5	8.4
Shape	–	Tangent ^{13}C	Tangent ^{13}C	Tangent ^{13}C	Tangent ^{13}C	Tangent ^{13}C
Carrier (ppm)	–	57	60.2	60.2	60.2	177.6
Time (ms)	20	4.0	5.0	6.0	5.5	5.5
Transfer 3				DREAM	MIRROR	MIRROR
Field (kHz)-^{1}H				115.3	21.6	22.1
Field (kHz)-^{13}C				8.3	–	–
Field (kHz)-^{15}N				–	–	–
Shape				Tangent ^{13}C	–	–
Carrier (ppm)				57	–	–
Time (ms)				4	25	20
t1 increments	768	980	640	112	96	96
Sweep width (t1) (kHz)	50	70	25	6	5	5
Acquisition time (t1) (ms)	7.7	7.0	12.9	9.3	9.6	9.6
t2 increments	2,048	2,048	2,048	80	144	144
Sweep width (t2) (kHz)	100	100	100	8	12	12
Acquisition time (t2) (ms)	10.2	10.2	10.2	5.0	6	6
t3 increments				1,536	2,048	2,048
Sweepwidth (t3) (kHz)				100	100	100
Acquisition time (t3) (ms)				7.7	10.2	10.2
^{1}H Spinal64 decoupling power (kHz)	100	100	100	100	100	100
Interscan delay (s)	2.5	2.0	2.2	2.2	2.3	2.3
Number of scans	20	16	40	8	16	8
Measurement time	11 h	9 h	16 h	2 days	6 days	3 days

b

Experiment	NCACX	NCOCX	CANCO	CCC	INEPT	CH/CH$_2$
MAS freq. (kHz)	17.5	17.5	17.5	17.5	17.5	18.0
Transfer 1	HN-CP	HN-CP	HC-CP	HC-CP	INEPT	HC-CP, n = 0
Field (kHz)-^{1}H	54.4	55.5	71.8	72.6	62.5	45
Field (kHz)-X	40.6	45.6	63.0	63.7	50	45
Shape	Tangent ^{1}H	Tangent ^{1}H	Tangent ^{1}H	Tangent ^{1}H	Hard pulses	
Carrier (ppm)	–	–	48.5	55.6	0	62.5
Time (ms)	0.8	1.0	0.5	0.5		0.7
Transfer 2	NC-CP	NC-CP	CN-CP	DREAM		HC-CP, n = 0
Field (kHz)-^{1}H	96	82	121	101.5		45
Field (kHz)-^{13}C	11.1	10.6	10.8	8.2		45

Table 1 continued

b

Experiment	NCACX	NCOCX	CANCO	CCC	INEPT	CH/CH_2
Field (kHz)-^{15}N	6.7	9.0	6.6	–		–
Shape	Tangent ^{13}C	Tangent ^{13}C	Tangent ^{13}C	Tangent ^{13}C		–
Carrier (ppm)	57.9	178.6	58.0	57.0		62.5
Time (ms)	5.0	5.0	8.0	4.0		0.278 (5× τ_r)
Transfer 3	DARR	DARR	NC-CP	DARR		DARR
Field (kHz)-^{1}H	11.8	7.5	110	3.4		11.8
Field (kHz)-^{13}C	–		10.8			–
Field (kHz)-^{15}N	–		8.1			–
Shape	–		Tangent ^{13}C			–
Carrier (ppm)	–		178.6			–
Time (ms)	80	80	6.0	200		100
t1 increments	80	72	128	248	192	1,024
Sweep width (t1) (kHz)	4	4	10	22	8	100
Acquisition (t1) (ms)	10.0	9.0	6.4	5.6	12.0	5.1
t2 increments	128	96	96	248	3,072	2,048
Sweep width (t2) (kHz)	10	8	4.8	22	100	100
Acquisition (t2) (ms)	6.4	6.0	10.0	5.6	15.4	10.3
t3 increments	2,048	2,048	2,048	2,048		
Sweepwidth (t3) (kHz)	100	100	100	100		
Acquisition (t3) (ms)	10.2	10.2	10.2	10.2		
^{1}H Spinal64 decoupling power (kHz)	100		100	100	77.8	100
Interscan delay (s)	2.2	2.2	2.35	1.9	2.5	2.2
Number of scans	16	16	8	4	8	8
Measurement time	4 days	3 days	3 days	6 days	1 h	13 h

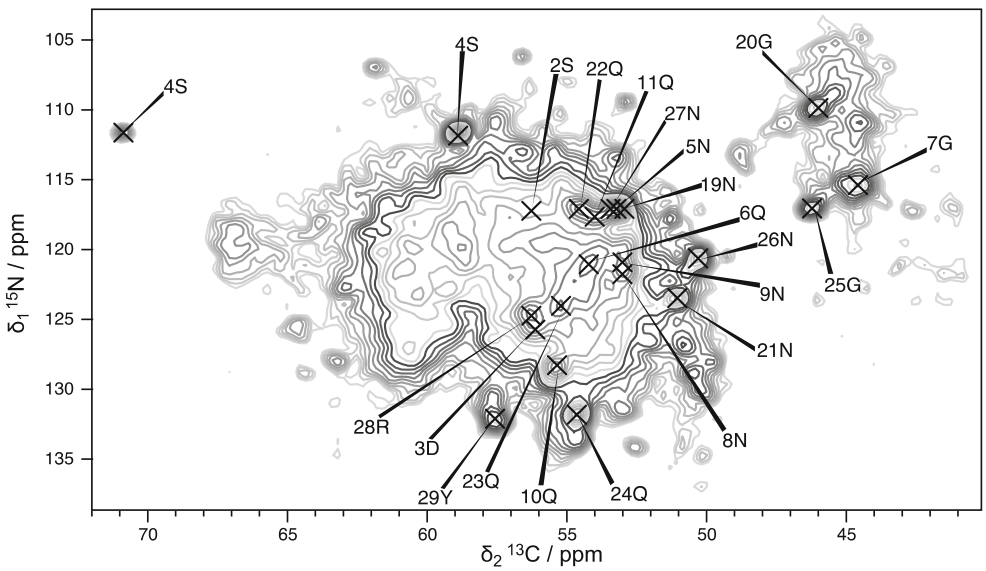

Fig. 2 2D NCA spectrum of Sup35p with labels for the sequentially assigned residues

connected via the sequential walk in NCACB/NCACO/NCACX to CANCO and to NCOCA/NCOCX spectra. Side-chain assignments were achieved using NCACB, NCACX, NCOCX and CCC spectra. Experimental details are given in Table 1. The spectra used for assignments were all recorded on a single sample, but several other

preparations were checked for reproducibility and yielded identical spectra.

All spectra were recorded on a Bruker Avance II+ 850 MHz spectrometer operating at a static field of 20 T. A 3.2 mm Bruker triple resonance MAS probe equipped with an LLC coil was used to reduce r.f. heating during the experiments. The spectra were recorded at sample temperatures of 7 °C. The pulse sequences were implemented as recently reported (Schuetz et al. 2010). All spectra were processed using TopSpin 2.0 (Bruker Biospin) by zero filling to no more than double the number of acquired points, the time domain signals were apodized with a squared cosine function (SSB 2.2–2.6 depending on spectrum and dimension). Spectra were analyzed and annotated using the CcpNmr Analysis package (Fogh et al. 2002; Vranken et al. 2005; Stevens et al. 2011).

Assignment and data deposition

The 2D NCA spectrum of Sup35p is shown in Fig. 2. The spectrum displays considerable overlap as can be expected for such a large protein. Many individual peaks are narrow however, as indicated by the isolated signals. One can already see in the 2D spectrum that there is a remarkably large distribution in peak intensities, and some isolated signals show higher intensities than crowded regions. Even stronger intensity variations are revealed in the 3D spectra (see Fig. 3 as an example), which actually show only a subset of the resonances observed in the 2D spectra; about 45 peaks can be counted in the NCACB spectrum. The linewidth of isolated correlations is mostly between 0.5 and 1 ppm (e.g. 0.6 ppm measured on Ser4 Cα and Cβ in the direct dimension), and the 3D spectra show a good resolution and dispersion, allowing for an assignment using the afore-mentioned 3D methods.

22 of the NCACB signals could be sequentially assigned to N, Cα, Cβ triples, and 3 to further side-chain resonances of the assigned residues. Assignments are given on the 2D NCA spectrum in Fig. 2.

To illustrate sequential assignments, a representative plane of the 3D NCACB, NCACO, CANCO and NCOCA experiments is shown in Fig. 3. The 22 assigned residues are all situated in the N-terminal portion of the prion domain. The chemical shifts have been deposited in the BMRB under the accession number 18407.

It might be noted that the Cβ chemical shift of Ser4 is atypically high with 70.9 ppm, which would rather correspond to the Cβ chemical shift of threonine. Nevertheless, several arguments do support this assignment. The sequential assignment of Ser4 is unambiguous in both directions towards Asp3 and Asn5. Furthermore, the signals observed

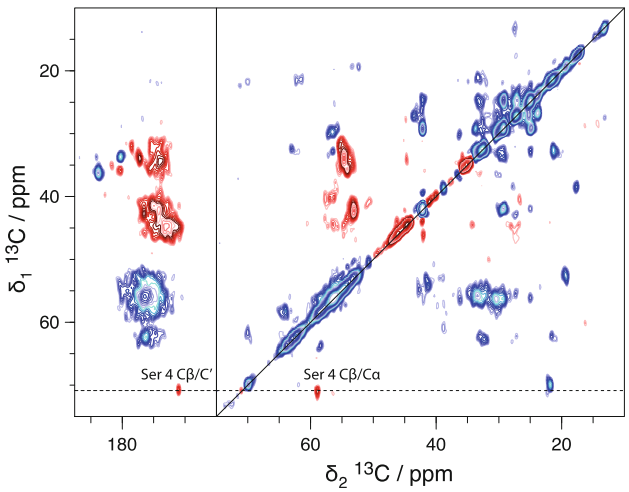

Fig. 4 CH versus CH_2 spectral editing for Sup35p. *Blue signals* correspond to positive contours and stem from CH or CH_3 groups (in δ_1). *Red signals* are negative and originate from CH_2 groups (see text). The Cβ–Cα and Cβ–C′ correlations of Ser4 have been labeled

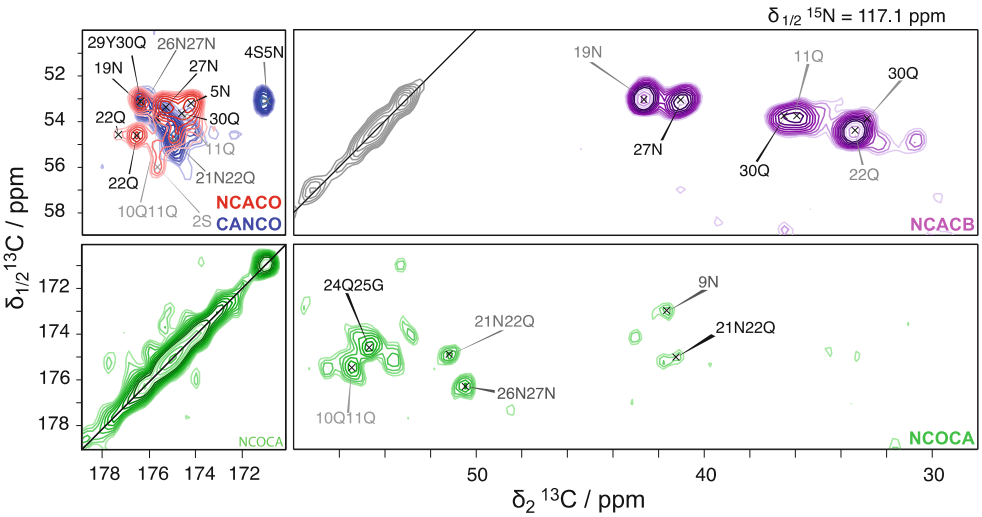

Fig. 3 Representative planes of the 3D NCC assignment spectra. Experimental details are given in Table 1. *NCACB* spectra are represented in *purple* (negative signals) and *grey* (positive signals), *NCACO* spectra in *red*, *CANCO* spectra in *blue* and *NCOCA* spectra in *green*. *Grey labels* are used if the resonance has a slightly different ^{15}N chemical shift than the represented plane

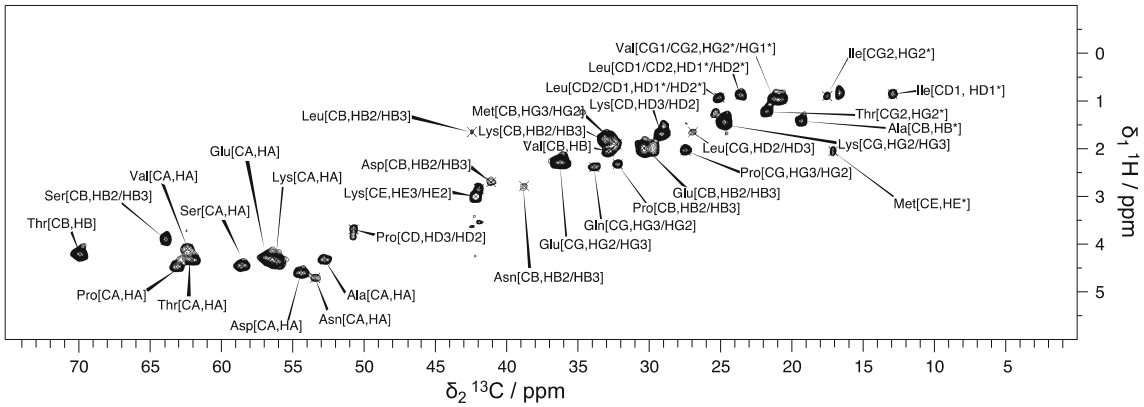

Fig. 5 INEPT spectrum of the Sup35 prion. The signals are assigned to residue types using the random coil chemical shifts (Wang and Jardetzky 2002)

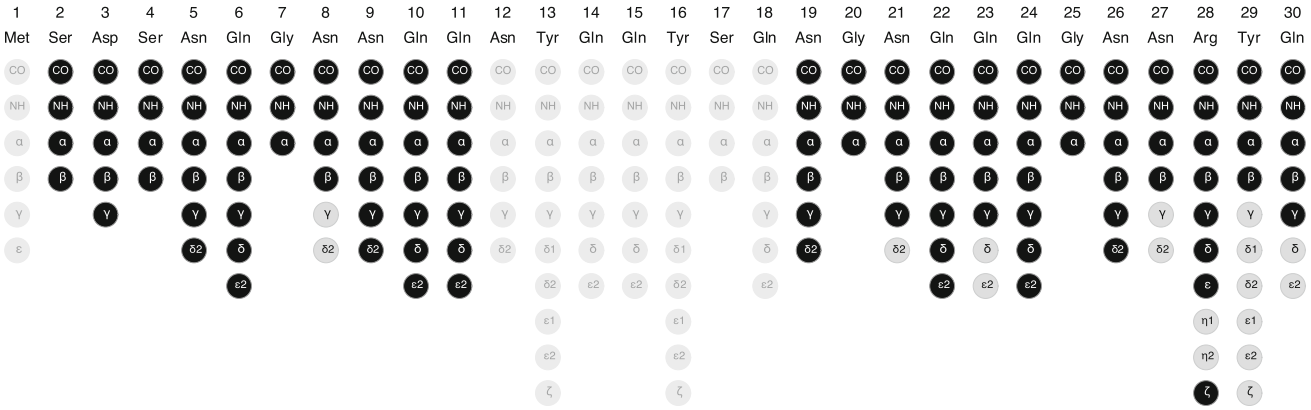

Fig. 6 Assignment graph created using the CCPNmr software (Fogh et al. 2002) of the N-terminal 30 amino acids of Sup35

in the spectra correspond to a serine spin system, since even at long DARR mixing times up to 200 ms no Cγ2 shift was observed in the ^{13}C–^{13}C-correlation spectra, although the Cα–Cβ correlation is generally one of the stronger peaks. Finally, in the BMRB 115 serine Cβ shifts outliers have been deposited (more than three sigma deviation from the average shift), reaching up to 76.4 ppm. A closer look at the PDB-deposited corresponding structures reveals that out of the 26 structures that show a Ser Cβ chemical shift above 70 ppm, more than 24 of the Ser are located in loops or unstructured regions. However, many of them lie just before or after a β-strand. The remaining two Ser are located at the beginning of a β-sheet. Since Ser4 is the first residue of a β-strand, as indicated by secondary chemical shifts (see below), this might be the reason for its unusually high Cβ chemical shift.

The assignment of Ser4 was verified independently by spectroscopic means using spectral editing techniques. In a Thr residue, the Cβ atom is part of a CH group, whereas it is part of a CH_2 group in a Ser residue. An approach for spectral editing of CH versus CH_2 groups in the solid state has been proposed (Wu and Zilm 1993; Sangill et al. 1994), which relies on the presence of second-order cross terms between ^{1}H–^{1}H and ^{1}H–^{13}C dipolar couplings in CH_2 groups. We have set up such an element followed by a DARR mixing time to resolve the signals in a 2D spectrum. An excerpt of the aliphatic region is shown in Fig. 4. The Cβ–Cα and Cβ–C′ correlations of Ser4 are inverted as would be expected for the CH_2 groups of Ser residues. One should note that the signal observed around 64/58 ppm corresponds to Ser random-coil chemical shifts, and thus stems from flexible residues. Their dipolar couplings are scaled and thus do not follow the editing rules for rigid residues. The inverted sign of the Ser4 correlations is another proof that despite the exotic Cβ chemical shift, the residue in question must be a Ser, and cannot be a Thr.

As mentioned above, parts of the protein show either static disorder or flexibility. Highly dynamic residues generally can be detected in INEPT spectra. All amino-acid types with the exception of Arg, Cys, Trp and Tyr could be observed in this scalar-coupling based spectrum as shown in Fig. 5. The absence of these residues in the spectra coincides with their absence in the M-domain. In addition, all residue-types present in the M-domain show signals in the INEPT spectrum.

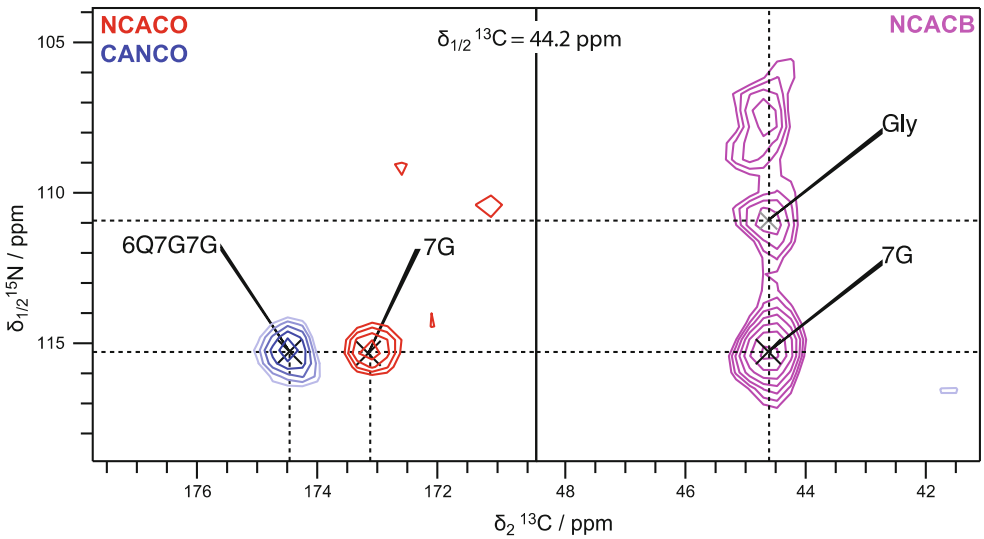

Fig. 7 Extract of *NCACB*, *NCACO*, and *CANCO* 3D spectra for Gly7 and an unassigned glycine residue. The absence of peaks in the *NCACO* and *CANCO* spectra shows that a sequential walk is not possible for this residue due to weak signal strength

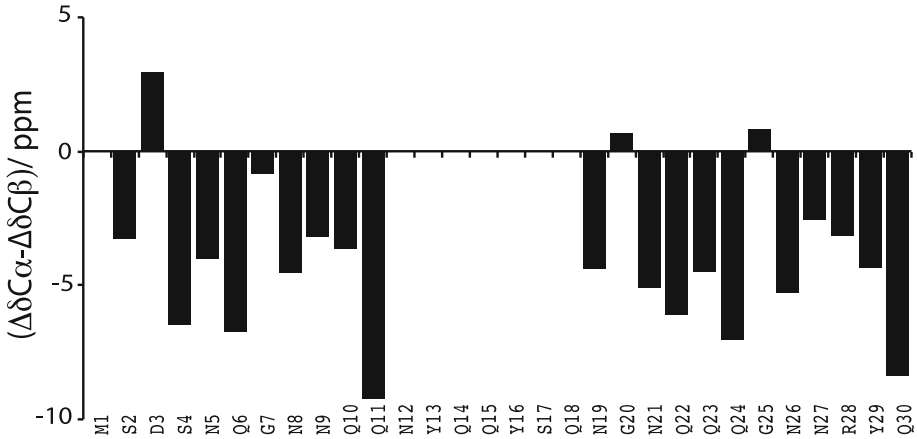

Fig. 8 Secondary chemical shifts for Sup35p. Secondary shifts have been calculated as described in (Wishart and Sykes 1994). Three or more negative values in a row suggest β-strand conformation. Isolated positive or negative values for a given residue suggest turn- or random coil-conformation. For Gly only the secondary shift of Cα is plotted

Assigned atoms are shown in the assignment graph in Fig. 6. Most strong cross peaks in the 2D NCA spectrum can be explained based on this assignment.

As mentioned above, assignments could not be obtained for all signals observed in the 3D spectra. A typical case of a signal present in the NCACB spectrum but not assignable due to absence of the corresponding peaks in the remaining 3D spectra is shown in Fig. 7, using the example of two glycine residues. In the more sensitive NCACB experiment, signals are observed for both glycines, however significantly weaker already for the upper one (labeled Gly). In the NCACO and CANCO spectra, shown in red and blue respectively, peaks are only observed for Gly7 and its connections to Gln6 (in the CANCO spectrum). For the other glycine, no signals allowing for sequential walk were detected.

The secondary chemical shifts for the assigned residues are given in Fig. 8. The assigned residues mostly display secondary chemical shifts typical for β-strand conformation, with the exception of residues Asp3 and Gly20 and Gly25.

To summarize, our data suggest that Sup35p possesses an amyloid core formed by two β-strands running from residues 2–11 and 19–30. Large parts of the remaining regions of the protein are statically disordered or show mobility on time scales that interfere with dipolar polarization transfer or that shorten the coherence lifetime. The sequential assignment of the strong signals observed in the Sup35p spectra constitutes a first step towards a high-resolution structure of its hypothetical amyloid core.

Acknowledgments We thank Dr. Christian Wasmer for help with recording the NMR spectra. This work was supported by the Agence Nationale de la Recherche (ANR-12-BS08-0013-01), the ETH Zurich, the Swiss National Science Foundation (Grant 200020_124611) and the Centre National de la Recherche Scientifique. We also acknowledge support from the European Commission under the Seventh Framework Programme (FP7), contract Bio-NMR 261863.

References

Böckmann A, Meier BH (2010) Prions: en route from structural models to structures. Prion 4(2):72–79

Böckmann A, Gardiennet C, Verel R, Hunkeler A, Loquet A, Pintacuda G, Emsley L, Meier BH, Lesage A (2009) Characterization of different water pools in solid-state NMR protein samples. J Biomol NMR 45(3):319–327

Comellas G, Lemkau LR, Nieuwkoop AJ, Kloepper KD, Ladror DT, Ebisu R, Woods WS, Lipton AS, George JM, Rienstra CM (2011) Structured regions of α-synuclein fibrils include the early-onset parkinsons disease mutation sites. J Mol Biol 411:881–895

Cox BS (1965) PSI, a cytoplasmic suppressor of super-suppressor in yeast. Heredity 20(4):505–521

Debelouchina GT, Platt GW, Bayro MJ, Radford SE, Griffin RG (2010) Magic angle spinning NMR analysis of beta(2)-microglobulin amyloid fibrils in two distinct morphologies. J Am Chem Soc 132(30):10414–10423

DePace AH, Santoso A, Hillner P, Weissman JS (1998) A critical role for amino-terminal glutamine/asparagine repeats in the formation and propagation of a yeast prion. Cell 93(7):1241–1252

Fitzpatrick AWP, Debelouchina GT, Bayro MJ, Clare DK, Caporini MA, Bajaj VS, Jaroniec CP, Wang L, Ladizhansky V, Müller SA, MacPhee CE, Waudby CA, Mott HR, De Simone A, Knowles TPJ, Saibil HR, Vendruscolo M, Orlova EV, Griffin RG, Dobson CM (2013) Atomic structure and hierarchical assembly of a cross-β amyloid fibril. Proc Natl Acad Sci USA 110:5468–5473

Fogh R, Ionides J, Ulrich E, Boucher W, Vranken W, Linge JP, Habeck M, Rieping W, Bhat TN, Westbrook J, Henrick K, Gilliland G, Berman H, Thornton J, Nilges M, Markley J, Laue E (2002) The CCPN project: an interim report on a data model for the NMR community. Nat Struct Biol 9(6):416–418

Gath J, Habenstein B, Bousset L, Melki R, Meier BH, Böckmann A (2012) Solid-state NMR sequential assignments of α-synuclein. Biomol NMR Assign 6(1):51–55

Habenstein B, Wasmer C, Bousset L, Sourigues Y, Schütz A, Loquet A, Meier BH, Melki R, Böckmann A (2011) Extensive de novo solid-state NMR assignments of the 33 kDa C-terminal domain of the Ure2 prion. J Biomol NMR 51(3):235–243

Heise H, Celej MS, Becker S, Riede D, Pelah A, Kumar A, Jovin TM, Baldus M (2008) Solid-state NMR reveals structural differences between fibrils of wild-type and disease-related A53T mutant alpha-synuclein. J Mol Biol 380(3):444–450

Krishnan R, Lindquist S (2005) Structural insights into a yeast prion illuminate nucleation and strain diversity. Nature 435(7043):765–772

Krzewska J, Melki R (2006) Molecular chaperones and the assembly of the prion Sup35p, an in vitro study. EMBO J 25(4):822–833

Krzewska J, Tanaka M, Burston SG, Melki R (2007) Biochemical and functional analysis of the assembly of full-length Sup35p and its prion-forming domain. J Biol Chem 282(3):1679–1686

Lewandowski JR, van der Wel PCA, Rigney M, Grigorieff N, Griffin RG (2011) Structural complexity of a composite amyloid fibril. J Am Chem Soc 133(37):14686–14698

Loquet A, Bousset L, Gardiennet C, Sourigues Y, Wasmer C, Habenstein B, Schütz A, Meier BH, Melki R, Böckmann A (2009) Prion fibrils of Ure2p assembled under physiological conditions contain highly ordered, natively folded modules. J Mol Biol 394(1):108–118

Loquet A, Giller K, Becker S, Lange A (2010) Supramolecular interactions probed by 13C–13C solid-state NMR spectroscopy. J Am Chem Soc 132(43):15164–15166

Luckgei N, Schütz AK, Bousset L, Habenstein B, Sourigues Y, Gardiennet C, Meier BH, Melki R, Böckmann A (2013a) The conformation of the prion domain of Sup35p in isolation and in the full-length protein is different (submitted)

Luckgei N, Schütz AK, Habenstein B, Bousset L, Sourigues Y, Melki R, Meier BH, Böckmann A (2013b) Solid-state NMR sequential assignments of the amyloid core of Sup35pN. doi:10.1007/s12104-013-9518-y

Nelson R, Sawaya M, Balbirnie M, Madsen A, Riekel C, Grothe R, Eisenberg D (2005) Structure of the cross-beta spine of amyloid-like fibrils. Nature 435(7043):773–778

Paravastu AK, Leapman RD, Yau W-M, Tycko R (2008) Molecular structural basis for polymorphism in Alzheimer's beta-amyloid fibrils. Proc Natl Acad Sci USA 105(47):18349–18354

Sangill R, Rastrupandersen N, Bildsoe H, Jakobsen HJ, Nielsen NC (1994) Optimized spectral editing of 13C MAS NMR spectra of rigid solids using cross-polarization methods. J Magn Reson A 107(1):67–78

Schuetz A, Wasmer C, Habenstein B, Verel R, Greenwald J, Riek R, Böckmann A, Meier BH (2010) Protocols for the sequential solid-state NMR spectroscopic assignment of a uniformly labeled 25 kDa protein: HET-s(1-227). Chembiochem 11(11):1543–1551

Shewmaker F, Wickner RB, Tycko R (2006) Amyloid of the prion domain of Sup35p has an in-register parallel beta-sheet structure. Proc Natl Acad Sci USA 103(52):19754–19759

Stansfield I, Jones K, Kushnirov V, Dagkesamanskaya A, Poznyakovski A, Paushkin S, Nierras C, Cox B, Teravanesyan M, Tuite M (1995) The products of the Sup45 (eRF1) and Sup35 genes interact to mediate translation termination in saccharomyces-cerevisiae. EMBO J 14(17):4365–4373

Stevens TJ, Fogh RH, Boucher W, Higman VA, Eisenmenger F, Bardiaux B, van Rossum B-J, Oschkinat H, Laue ED (2011) A software framework for analysing solid-state MAS NMR data. J Biomol NMR 51(4):437–447

Toyama B, Kelly M, Gross J, Weissman J (2007) The structural basis of yeast prion strain variants. Nature 449(7159):233–237

Tycko R (2006) Solid-state NMR as a probe of amyloid structure. Protein Pept Lett 13:229–234

van der Wel PC, Hu K, Lewandowski JR, Griffin RG (2006) Dynamic nuclear polarization of amyloidogenic peptide nanocrystals: GNNQQNY, a core segment of the yeast prion protein Sup35p. J Am Chem Soc 128(33):10840–10846

van der Wel PCA, Lewandowski JR, Griffin RG (2007) Solid-state NMR study of amyloid nanocrystals and fibrils formed by the peptide GNNQQNY from yeast prion protein Sup35p. J Am Chem Soc 129(16):5117–5130

van der Wel PCA, Lewandowski JR, Griffin RG (2010) Structural characterization of GNNQQNY amyloid fibrils by magic angle spinning NMR. Biochemistry 49(44):9457–9469

van Melckebeke H, Wasmer C, Lange A, Ab E, Loquet A, Böckmann A, Meier BH (2010) Atomic-resolution three-dimensional structure of HET-s(218–289) amyloid fibrils by solid-state NMR spectroscopy. J Am Chem Soc 132(39):13765–13775

Vranken W, Boucher W, Stevens T, Fogh R, Pajon A, Llinas P, Ulrich E, Markley J, Ionides J, Laue E (2005) The CCPN data model for NMR spectroscopy: development of a software pipeline. Proteins 59(4):687–696

Wang Y, Jardetzky O (2002) Probability-based protein secondary structure identification using combined NMR chemical-shift data. Protein Sci 11(4):852–861

Wasmer C, Lange A, van Melckebeke H, Siemer AB, Riek R, Meier BH (2008) Amyloid fibrils of the HET-s(218–289) prion form a beta solenoid with a triangular hydrophobic core. Science 319(5869):1523–1526

Wickner RB, Masison DC, Edskes HK (1995) [PSI] and [URE3] as yeast prions. Yeast 11(16):1671–1685

Wishart DS, Sykes BD (1994) The 13C chemical-shift index: a simple method for the identification of protein secondary structure using 13C chemical-shift data. J Biomol NMR 4(2):171–180

Wu X, Zilm K (1993) Complete spectral editing in CPMAS NMR. J Magn Reson A 102(2):205–213